

## Environmental Nonadditivity and Franck-Condon physics in Nonequilibrium Quantum Systems

Henry Maguire,<sup>1</sup> Jake Iles-Smith,<sup>1,2</sup> and Ahsan Nazir<sup>1</sup>

<sup>1</sup>*Photon Science Institute & School of Physics and Astronomy, The University of Manchester, Oxford Road, Manchester M13 9PL, United Kingdom*

<sup>2</sup>*Department of Physics and Astronomy, University of Sheffield, Hounsfield Road, Sheffield, S3 7RH, United Kingdom*

 (Received 8 January 2019; published 28 August 2019; corrected 27 May 2020)

We show that for a quantum system coupled to both vibrational and electromagnetic environments, enforcing additivity of their combined influences results in nonequilibrium dynamics that does not respect the Franck-Condon principle. We overcome this shortcoming by employing a collective coordinate representation of the vibrational environment, which permits the derivation of a nonadditive master equation. When applied to a two-level emitter our treatment predicts decreasing photon emission rates with increasing vibrational coupling, consistent with Franck-Condon physics. In contrast, the additive approximation predicts the emission rate to be completely insensitive to vibrations. We find that nonadditivity also plays a key role in the stationary nonequilibrium model behavior, enabling two-level population inversion under incoherent electromagnetic excitation.

DOI: 10.1103/PhysRevLett.123.093601

The Franck-Condon (FC) principle [1,2] is an invaluable tool in the study of solid-state and molecular emitters. The principle states that electronic transitions of an emitter occur without changes to the motions of its nuclei or those of its environment. As a result, transition rates become dependent on the overlap between vibrational configurations in the initial and final states, which are generally displaced from one another [see Fig. 1(a)]. This picture provides an intuitive starting point for studying the complex interactions between the electronic and vibrational degrees of freedom of an emitter and its environment, for example, through rate equations derived from Fermi's golden rule [1,2].

Faithfully representing the full nonequilibrium dynamics of such systems requires moving beyond rate equations and instead employing an explicitly time-dependent approach. This should be nonperturbative in the electron-vibrational coupling and thus capable of capturing the dynamical influence of vibrational displacement on the electronic states. Examples include polaron [3,4] and collective coordinate [5–7] master equations, hierarchical equations of motion [8–10], path integrals [11–13], and tensor network methods [14–16]. Nevertheless, it is interactions with the electromagnetic environment that ultimately give rise to the observed electronic (e.g., optical) transitions. Our focus is thus on the important question of how to incorporate electromagnetic interactions into the dynamical formalism, such that they respect the nonperturbative nature of the vibrational coupling.

Given that interactions with the electromagnetic field in free space are weak, it is often assumed that the Markovian

dynamics they generate can be added to the equations of motion unmodified due to the presence of vibrations [17–32]. Though justifiable in certain circumstances [22,33–36], additivity is, in general, a stringent requirement [35–39] that can break down even if all environments are weakly coupled to the system [37]. In fact, we shall show below that the dynamics obtained in this manner can exhibit fundamental flaws, such as disregarding the FC principle.

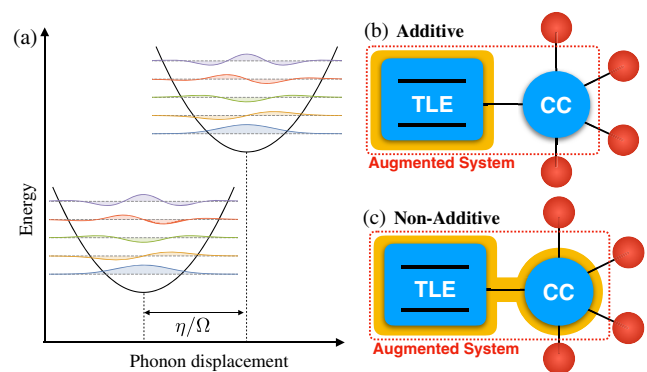


FIG. 1. (a) Illustration of the vibronic energy structure commonly associated to the Franck-Condon principle. Vibrational coupling leads to the formation of manifolds corresponding to the ground and excited electronic configurations, with transition probabilities proportional to the overlap of the displaced and undisplaced vibrational states. (b),(c) Schematics of the collective coordinate mapping. In the additive case (b) the electromagnetic field (shaded) is sensitive only to the two-level emitter (TLE), whereas in the nonadditive case (c) it is sensitive to the full augmented system (TLE + CC).

In certain cases, both the vibrational and electromagnetic environments may be treated nonperturbatively [40,41], but this comes at an inevitable cost in terms of computational effort and complexity within the formalism.

Here we seek to retain both the simplicity of the Markovian description of the electromagnetic interactions and a nonperturbative treatment of the electron-vibrational coupling, but without the undesirable additivity restriction. This is made possible through a collective coordinate (CC) transformation [5,7,42,43], which incorporates nonperturbative effects of the vibrational environment into an enlarged (augmented) system [see Figs. 1(b),1(c)]. This in turn enables a Markovian master equation to be derived in the eigenbasis of the augmented system space, rather than that of the original bare emitter, by tracing out the electromagnetic environment and residual vibrational modes [7]. On doing so we find that electromagnetic transitions become sensitive to the nonperturbative vibrational dynamics captured by the CC mapping, and our procedure thus retains the nonadditive effects crucial to obtaining quantum dynamics that are consistent with the FC principle [Fig. 1(c)]. If instead we enforce additivity [Fig. 1(b)], the resulting electronic decay dynamics becomes independent of the electron-vibrational coupling. We show that capturing nonadditivity is also vital for accurately representing the stationary nonequilibrium behavior within our model. Specifically, under incoherent electromagnetic excitation the nonadditive interplay between the electromagnetic field and vibrations directly enables electronic population inversion for situations impossible within the additive approach.

Before examining nonequilibrium dynamics explicitly, we can illustrate the shortcomings of an additive approximation through arguments based on a simple Fermi golden rule calculation. We consider a two-level molecular emitter (a monomer) with electronic excited state  $|e\rangle$  and ground state  $|g\rangle$ , separated by an energy  $\epsilon$  ( $\hbar = 1$  throughout). Coupling to the electromagnetic field induces transitions between the electronic states, which are also assumed to couple with strength  $\eta$  to a single (harmonic) vibrational mode of frequency  $\Omega$ , leading to the formation of a displaced manifold associated to the excited electronic configuration. This is the situation depicted qualitatively in Fig. 1(a), though our considerations here and throughout the rest of the Letter also apply in the case of continuum phonon environments, where the discrete mode would be identified as the CC post mapping (see below).

We assume for the purpose of calculating the rate that shortly after excitation the system has relaxed to thermal equilibrium in the excited state manifold,  $\rho_{\text{eq}} = \sum_m p_m |e, \tilde{m}\rangle \langle e, \tilde{m}|$ , where  $p_m = e^{-m\Omega/k_B T} / \sum_n e^{-n\Omega/k_B T}$  with temperature  $T$ , and the displaced vibrational basis is denoted  $|\tilde{m}\rangle = D(\eta/\Omega)|m\rangle$  for the vibrational Fock state  $|m\rangle$  and displacement operator  $D(\alpha)$ . From Fermi's golden rule the electronic excited to ground state decay rate is then [1]

$$\Gamma_{e \rightarrow g} = \sum_{n,m} p_n \mathcal{J}(\Delta\omega_{\tilde{m},n}) |\langle \tilde{m}|n\rangle|^2. \quad (1)$$

There are two principal components to this expression. One is the overlap between vibrational configurations,  $|\langle \tilde{m}|n\rangle|^2$ , which is known as the FC factor. The other is the electromagnetic spectral density  $\mathcal{J}(\omega)$ . This describes the system-field coupling strength weighted by the electromagnetic density of states, and should be sampled at all energy differences between relevant states in the excited and ground manifolds,  $\Delta\omega_{\tilde{m},n}$ . In the additive approximation, however, the electromagnetic field coupling is treated in isolation from the vibrational interactions, and the electromagnetic spectral density is then incorrectly sampled only at the single frequency  $\epsilon$  corresponding to the bare electronic ground and excited state splitting. The expression for the emission rate then reduces to  $\Gamma_{e \rightarrow g} \approx \mathcal{J}_0 \sum_n |\langle \tilde{0}|n\rangle|^2 = \mathcal{J}_0$ , where  $\mathcal{J}_0 = \mathcal{J}(\epsilon)$  and we have used  $\sum_n |n\rangle \langle n| = \mathbb{1}$ . Thus, in the additive case the FC factor vanishes, and the transition rate loses its dependence on the electron-vibrational coupling. Note that this reasoning can be used to show that the flat spectral density approximation commonly used in quantum optics theory [44] also fails in regimes of strong coupling to vibrational modes.

We now develop a microscopic description in order to establish the extent to which nonadditivity can influence the quantum dynamics of electron-vibrational models beyond the heuristic arguments outlined above. Our Hamiltonian is written as  $H = H_S + H_I + H_B$ , with system Hamiltonian  $H_S = \epsilon|e\rangle \langle e|$ . The electronic configuration of the emitter molecule is directly influenced by both vibrational and electromagnetic environments, such that  $H_I = H_I^{\text{PH}} + H_I^{\text{EM}}$ . Within the harmonic approximation the electron-vibrational coupling is written

$$H_I^{\text{PH}} = |e\rangle \langle e| \otimes \sum_k g_k (b_k^\dagger + b_k) + |e\rangle \langle e| \sum_k \frac{g_k^2}{\nu_k}, \quad (2)$$

where  $b_k$  is the annihilation operator for the  $k$ th phonon mode and the second term shifts the excited state due to the reorganization energy associated to vibrational displacement. The coupling to the phonon environment is characterized by its spectral density, for which we take the common form  $J(\nu) = \sum_k |g_k|^2 \delta(\nu - \nu_k) = \alpha \nu_0^2 \gamma \nu / [(\nu^2 - \nu_0^2)^2 + \gamma^2 \nu^2]$ . Here  $\alpha$  and  $\nu_0$  define the coupling strength and peak position, respectively, and  $\gamma$  controls whether  $J(\nu)$  is narrow (underdamped) or broad (overdamped) [6,45]. In addition to the phonon environment, we also have an explicit coupling to the electromagnetic field, given by  $H_I^{\text{EM}} = -\mathbf{d} \cdot \mathbf{E}$  in the dipole approximation, where  $\mathbf{d}$  is the emitter dipole operator and  $\mathbf{E}$  is the electric field operator [46–48]. Ignoring polarization degrees of freedom and working in the rotating wave approximation, this then takes the form

$$H_I^{\text{EM}} = \sum_l (f_l \sigma^\dagger a_l + f_l^* \sigma a_l^\dagger), \quad (3)$$

where  $\sigma = |g\rangle\langle e|$  and  $a_l$  is the annihilation operator for the  $l$ th mode of the electromagnetic field. The spectral density for the light-matter coupling is defined as  $\mathcal{J}(\omega) = \sum_l |f_l|^2 \delta(\omega - \omega_l) = (2\pi\epsilon^3)^{-1} \Gamma_0 \omega^3$  [46–48], where  $\Gamma_0$  is the spontaneous emission rate for the two-level emitter in the absence of phonons. Finally,  $H_B = H_B^{\text{EM}} + H_B^{\text{PH}} = \sum_l \omega_l a_l^\dagger a_l + \sum_k \nu_k b_k^\dagger b_k$  is the sum of the internal Hamiltonians for the electromagnetic and vibrational environments.

Applying a CC mapping to the phonon bath allows us to incorporate its influence on the electronic dynamics nonperturbatively, and, in particular, to capture the resulting dynamical generation of electron-vibrational correlations [5,6,42,43]. Our Hamiltonian maps as  $H = H_S + H_I + H_B \rightarrow H'_S + H'_I + H_I^{\text{EM}} + H'_B + H_B^{\text{EM}}$ , which leaves the light-matter coupling unchanged. Here, we have introduced the transformed Hamiltonians

$$H'_S = H_S + \eta |e\rangle\langle e| (b^\dagger + b + \pi\alpha/2\eta) + \Omega b^\dagger b, \quad (4)$$

$$H'_I = (b^\dagger + b) \sum_m h_m (c_m^\dagger + c_m) + (b^\dagger + b)^2 \sum_m \frac{h_m^2}{\tilde{\nu}_m}, \quad (5)$$

$$H'_B = \sum_m \tilde{\nu}_m c_m^\dagger c_m, \quad (6)$$

where  $b + b^\dagger = \sum_k g_k (b_k^\dagger + b_k)/\eta$  defines creation and annihilation operators for the CC,  $c_m$  is the annihilation operator for the  $m$ th mode of the residual environment to which it couples, and we have expressed the reorganization energy as  $\sum_k g_k^2/\nu_k = \int_0^\infty d\nu J(\nu)/\nu = \pi\alpha/2$ . The CC parameters can be written in terms of the quantities defining the vibrational spectral density:  $\eta^2 = \pi\alpha\nu_0/2$  and  $\Omega = \nu_0$  [6]. Coupling between the augmented emitter-CC system and the residual phonon environment is described by an Ohmic spectral density  $J_R(\nu) = \sum_m |h_m|^2 \delta(\nu - \tilde{\nu}_m) = \gamma\nu/2\pi\nu_0$  [6], and ensures that the vibrational environment still acts as a continuum of modes after the mapping. As in the single mode case discussed earlier, the coupling to the CC leads to the formation of two vibronic manifolds associated with the ground and excited electronic configurations. The coupling to the residual environment induces transitions *within* each vibronic manifold. This leads both to broadening and to dynamical relaxation of the phonon environment, which typically occurs on a subpicosecond timescale.

From the mapped Hamiltonian we derive a second-order Born-Markov master equation by tracing over the residual environment and the electromagnetic field [47], both of which are assumed to remain in thermal equilibrium at temperatures  $T_R$  and  $T_{\text{EM}}$ , respectively:  $\rho_i = e^{-H_i/k_B T_i} / \text{tr}[e^{-H_i/k_B T_i}]$ , for  $i = R, \text{EM}$ . The resulting master equation can be written  $\partial_t \rho(t) = \mathcal{L}[\rho(t)]$  with Liouvillian [49]:

$$\mathcal{L}[\rho(t)] = -i[H'_S, \rho(t)] + \mathcal{K}_R[\rho(t)] + \mathcal{K}_{\text{EM}}[\rho(t)], \quad (7)$$

where  $\rho(t)$  is the reduced state of the augmented emitter-CC system. Here,  $\mathcal{K}_R$  is a superoperator representing the action of the residual phonon environment [6]:

$$\mathcal{K}_R[\rho(t)] = [S, \rho(t)\zeta] + [\zeta^\dagger \rho(t), S], \quad (8)$$

with  $S = b^\dagger + b$  and

$$\zeta = \frac{\pi}{2} \sum_{jk} J_R(\lambda_{jk}) \left[ \coth\left(\frac{\lambda_{jk}}{2k_B T_R}\right) + 1 \right] S_{jk} |\psi_j\rangle\langle\psi_k|, \quad (9)$$

where the eigenbasis of the augmented system is defined through  $H'_S |\psi_j\rangle = \psi_j |\psi_j\rangle$ , giving  $\lambda_{jk} = \psi_j - \psi_k$  and  $S_{jk} = \langle\psi_j|S|\psi_k\rangle$ . We solve for the eigenvalues  $\psi_j$  and eigenstates  $|\psi_j\rangle$  numerically, taking the basis  $\{|g\rangle, |e\rangle\}$  for the TLE and a Fock (number) state basis for the CC.

The effects of the electromagnetic field interaction are contained within  $\mathcal{K}_{\text{EM}}$ . Importantly, the augmented emitter-CC system Hamiltonian,  $H'_S$ , is treated (numerically) exactly within the formalism. This is crucial in capturing nonadditive effects of the electromagnetic and vibrational environments, as it means that when we move the electromagnetic interaction Hamiltonian [Eq. (3)] into the interaction picture, we do so with respect to the full augmented system Hamiltonian  $H'_S$  [Eq. (4)]. The mapping thus ensures that the electromagnetic environment is sensitive to the underlying eigenstructure of both the electronic and vibrational states. The superoperator representing the dynamical influence of the electromagnetic environment then takes the form (see the Supplemental Material [49] for full details)

$$\mathcal{K}_{\text{EM}}[\rho(t)] = -[\sigma^\dagger, \chi_1 \rho(t)] - [\sigma, \chi_2 \rho(t)] + \text{H.c.}, \quad (10)$$

where we have introduced the rate operators describing decay from the excited to the ground vibronic manifold,  $\chi_1 = \sum_{jk} \sigma_{jk} \Gamma_\downarrow(\lambda_{jk}) |\psi_j\rangle\langle\psi_k|$ , and absorption in the opposite direction,  $\chi_2 = \sum_{jk} \sigma_{jk}^* \Gamma_\uparrow(\lambda_{jk}) |\psi_k\rangle\langle\psi_j|$ , with transition rates given by  $\Gamma_\downarrow(\lambda) = \pi \mathcal{J}(\lambda) (n(\lambda) + 1)$  and  $\Gamma_\uparrow(\lambda) = \pi \mathcal{J}(\lambda) n(\lambda)$ , for field occupation number  $n(\lambda) = [\exp(\lambda/k_B T_{\text{EM}}) - 1]^{-1}$  and  $\sigma_{jk} = \langle\psi_j|\sigma|\psi_k\rangle$ . From these expressions, it is evident that the interaction between the system and the electromagnetic field is dependent on the eigenstructure of the augmented system, and thus on the emitter-vibrational coupling through the identification of the CC, and its coupling to the electronic system. We therefore refer to this theory as being *nonadditive*.

In contrast, within the additive approach  $\mathcal{K}_{\text{EM}}$  is derived without reference to the vibrational coupling. In the present setting, this amounts to neglecting the modification of the system eigenstructure due to vibrational interactions encoded in the mapped system Hamiltonian  $H'_S$ ,

and instead moving the electromagnetic interaction Hamiltonian [Eq. (3)] into the interaction picture with respect to the original system Hamiltonian  $H_S$ . This results in the standard Lindblad dissipator common in quantum optics theory:  $\mathcal{K}_{\text{EM}}[\rho(t)] = (\Gamma_0/2)[n(\epsilon) + 1]\mathcal{L}_\sigma[\rho(t)] + (\Gamma_0/2)n(\epsilon)\mathcal{L}_{\sigma^\dagger}[\rho(t)]$ , where  $\mathcal{L}_O[\rho] = 2O\rho O^\dagger - \{O^\dagger O, \rho\}$ . It is thus clear that within the additive approximation the electromagnetic field superoperator loses its explicit dependence on the vibrational environment. For vanishing electromagnetic interactions ( $\Gamma_0 \rightarrow 0$ ), the additive and nonadditive theories become equivalent and the problem reduces to the independent boson model, for which an exact solution can be obtained. We verify that the CC master equation agrees with this exact solution for a range of parameters in the Supplemental Material [49].

We are now in a position to investigate the impact of nonadditive effects on the dynamics of our model system. We begin by considering the decay of an emitter initialized in its excited state with the collective coordinate in a thermal state set by the residual bath temperature  $T_R$ :  $\rho(0) = |e\rangle\langle e| \otimes \rho_{\text{th}}$ , where  $\rho_{\text{th}} = \exp(-\Omega b^\dagger b/k_B T_R)/\text{tr}[\exp(-\Omega b^\dagger b/k_B T_R)]$ . This approximates a canonical thermal state of the original vibrational Hamiltonian in the unmapped representation at the same temperature, and is thus consistent with rapid (vertical) excitation of the system whereby the electronic state changes suddenly but the vibrational states remain unchanged. The vibrational environment will subsequently relax towards the displaced thermal state associated with the excited state manifold, captured dynamically within our approach. For concreteness, we consider an emitter splitting within the visible range and a vibrational spectral density peaked around a typical value for modes of certain dye molecules [50,51], polymers [52], and photosynthetic complexes [53,54].

Figure 2(a) shows the emitter excited state population dynamics predicted by the additive (dotted) and nonadditive (solid) theories for increasing electron-phonon coupling at ambient temperature. Both theories give rise to exponential decay, with the rate in the additive theory remaining constant across all electron-phonon coupling strengths. The nonadditive theory, in contrast, displays a monotonic decrease in the decay rate with increasing phonon coupling. This can be seen explicitly in Fig. 2(b), where we extract the decay rates directly from the master equation. Specifically, the excited to ground state transition rate can be written as

$$\Gamma_{e \rightarrow g} = \sum_n \langle g, n | \mathcal{L}[\rho_X(0)] | g, n \rangle, \quad (11)$$

with the Liouvillian taken to be additive or nonadditive depending on which case is under investigation. Here we must modify the initial state to account for the aforementioned rapid residual bath induced relaxation of the CC to a displaced thermal state prior to emission:  $\rho_X(0) = |e\rangle\langle e| \otimes e^{-X}\rho_{\text{th}}e^X$ , where  $X = \Omega^{-1}\eta(b^\dagger - b)$ . As expected, the rate from the additive theory displays no variation with

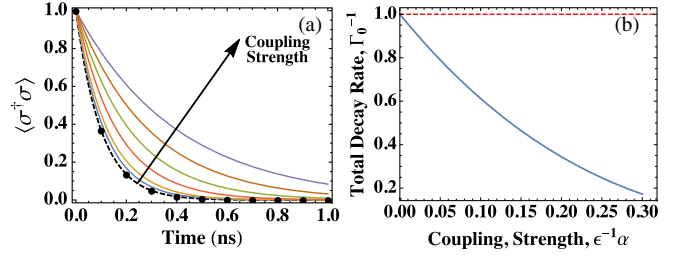


FIG. 2. (a) Emitter population dynamics from the additive (dots) and nonadditive (solid) theories for increasing vibrational coupling strength  $\epsilon^{-1}\alpha = 0.025, 0.05, 0.1, 0.15, 0.2, \text{ and } 0.25$ . The nonadditive theory shows a steady reduction of the decay rate for increasing coupling, whereas within the additive theory the rate remains constant (i.e., all dotted curves lie on top of each other). (b) Excited to ground state emission rate against vibrational coupling strength from the additive (dashed) and nonadditive (solid) theories in units of the bare decay rate  $\Gamma_0$ . Parameters:  $\epsilon = 2$  eV,  $\nu_0 = 50$  meV,  $\gamma = 10$  meV,  $\Gamma_0^{-1} = 100$  ps, and  $T_R = T_{\text{EM}} = 300$  K.

phonon coupling strength, in line with the simple golden rule calculation discussed previously but at odds with the FC principle. This again highlights deficiencies with the phenomenological additive treatment of the electromagnetic field. Conversely, the nonadditive theory shows a steady reduction of the emission rate as a function of phonon coupling, consistent with FC physics. As the displacement between the ground and excited state manifolds increases linearly with the electron-phonon coupling strength, this reduces the overlap between the vibrational states and thus suppresses electromagnetic transitions.

It is important to stress that discrepancies between the additive and nonadditive treatments in our model extend further than spontaneous emission processes. For example, we now consider situations in which the emitter is driven incoherently via thermal occupation of the electromagnetic environment at increased temperature  $T_{\text{EM}}$ , which constitutes an important building block of widely used models for natural and artificial solar energy conversion. Figure 3(a) shows the steady state population of the electronic excited state as a function of electron-phonon coupling strength, where the additive treatment once again displays no variation, simply matching the equilibrium distribution expected in the absence of vibrations. The nonadditive treatment, on the other hand, shows a monotonic increase in the steady state population of the excited state manifold. Most strikingly, at large coupling strengths there emerges a steady state population inversion. In the absence of phonons, such an inversion would be impossible, with emission and absorption processes balancing each other in equilibrium. This remains true in the presence of phonons when the electromagnetic field is treated additively, as highlighted in Fig. 3(b). Here, the additive theory approaches, but never exceeds, a maximum steady state population  $\langle \sigma^\dagger \sigma \rangle = 0.5$  in the limit of very large temperatures. In contrast, within the

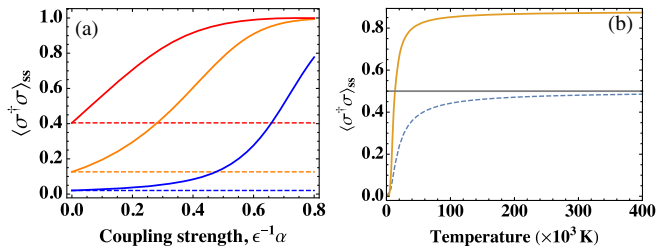


FIG. 3. (a) Steady-state emitter population as a function of the electron-phonon coupling strength for the additive (dashed) and nonadditive (solid) theories. The electromagnetic field temperatures are  $T_{EM} = 6000$  (blue, lower), 12 000 (orange, middle), and 60 000 K (red, upper). (b) Steady-state emitter population with varying temperature for  $\alpha = 0.3e$  from the additive (dashed) and nonadditive (solid) theories. In the additive theory the stationary population asymptotically approaches 0.5 (gray line) and never displays an inversion, in contrast to the nonadditive treatment. Other parameters are as in Fig. 2.

nonadditive theory, cooperative effects between the electromagnetic and vibrational environments lead to nonequilibrium stationary states that display substantial levels of population inversion. That such effects should be possible, even for continuum environments, is made clear from the CC mapping. Within the nonadditive theory the electromagnetic field has access to the full vibrational structure of the emitter, providing the necessary states to drive a population inversion. This points to a crucial difference between nonadditive and additive treatments, where disregarding the eigenstructure of the combined electronic and vibrational system misses key aspects of the nonequilibrium physics.

In summary, we have demonstrated that for models of electronic systems strongly coupled to vibrational environments, including the electromagnetic field in an additive manner can lead to dynamics inconsistent with the FC principle. By developing a dynamical formalism based on collective coordinate mappings, we capture the impact of nonadditive effects to recover both transient and stationary nonequilibrium behavior consistent with FC physics. Furthermore, we find that for common model assumptions on the forms of vibrational and electromagnetic couplings, nonadditive phenomena enable steady-state population inversion under incoherent electromagnetic excitation conditions. It would be interesting to explore whether such inversions could be harnessed to enhance work extraction (i.e., current) in models of solar energy conversion devices.

The authors wish to thank Adam Stokes and Neill Lambert for useful discussions. H.M. is supported by the EPSRC. A.N. and J.I.S. are supported by the EPSRC, Grant No. EP/N008154/1. J.I.S. also acknowledges support from the Royal Commission for the Exhibition of 1851.

- [1] V. May and O. Kühn, *Charge and Energy Transfer Dynamics in Molecular Systems* (Wiley, New York, 2004).
- [2] A. Nitzan, *Chemical Dynamics in Condensed Phases* (Oxford University Press, Oxford, 2006).
- [3] S. Jang and Y.-C. Cheng, *WIREs Comput. Mol. Sci.* **3**, 84 (2012).
- [4] A. Nazir and D. P. S. McCutcheon, *J. Phys. Condens. Matter* **28**, 103002 (2016).
- [5] J. Iles-Smith, N. Lambert, and A. Nazir, *Phys. Rev. A* **90**, 032114 (2014).
- [6] J. Iles-Smith, A. G. Dijkstra, N. Lambert, and A. Nazir, *J. Chem. Phys.* **144**, 044110 (2016).
- [7] M. Wertnik, A. Chin, F. Nori, and N. Lambert, *J. Chem. Phys.* **149**, 084112 (2018).
- [8] Y. Tanimura and R. Kubo, *J. Phys. Soc. Jpn.* **58**, 101 (1989).
- [9] A. Ishizaki and Y. Tanimura, *J. Phys. Soc. Jpn.* **74**, 3131 (2005).
- [10] A. Ishizaki and G. R. Fleming, *J. Chem. Phys.* **130**, 234111 (2009).
- [11] N. Makri and D. E. Makarov, *J. Chem. Phys.* **102**, 4600 (1995).
- [12] N. Makri and D. E. Makarov, *J. Chem. Phys.* **102**, 4611 (1995).
- [13] P. Nalbach, D. Braun, and M. Thorwart, *Phys. Rev. E* **84**, 041926 (2011).
- [14] R. Rosenbach, J. Cerrillo, S. F. Huelga, J. Cao, and M. B. Plenio, *New J. Phys.* **18**, 023035 (2016).
- [15] F. A. Y. N. Schröder and A. W. Chin, *Phys. Rev. B* **93**, 075105 (2016).
- [16] A. Strathearn, P. Kirton, D. Kilda, J. Keeling, and B. W. Lovett, *Nat. Commun.* **9**, 3322 (2018).
- [17] C. Kreisbeck, T. Kramer, M. Rodríguez, and B. Hein, *J. Chem. Theory Comput.* **7**, 2166 (2011).
- [18] A. G. Dijkstra and Y. Tanimura, *New J. Phys.* **14**, 073027 (2012).
- [19] F. Fassio, A. Olaya-Castro, and G. D. Scholes, *J. Phys. Chem. Lett.* **3**, 3136 (2012).
- [20] P. Kaer, T. R. Nielsen, P. Lodahl, A.-P. Jauho, and J. Mørk, *Phys. Rev. B* **86**, 085302 (2012).
- [21] A. Ulhaq, S. Weiler, C. Roy, S. M. Ulrich, M. Jetter, S. Hughes, and P. Michler, *Opt. Express* **21**, 4382 (2013).
- [22] D. P. S. McCutcheon and A. Nazir, *Phys. Rev. Lett.* **110**, 217401 (2013).
- [23] R. Betzholtz, J. M. Torres, and M. Bienert, *Phys. Rev. A* **90**, 063818 (2014).
- [24] N. Killoran, S. F. Huelga, and M. B. Plenio, *J. Chem. Phys.* **143**, 155102 (2015).
- [25] H.-B. Chen, P.-Y. Chiu, and Y.-N. Chen, *Phys. Rev. E* **94**, 052101 (2016).
- [26] A. M. Barth, A. Vagov, and V. M. Axt, *Phys. Rev. B* **94**, 125439 (2016).
- [27] M. Qin, H. Z. Shen, X. L. Zhao, and X. X. Yi, *Phys. Rev. A* **96**, 012125 (2017).
- [28] R. Stones, H. Hossein-Nejad, R. van Grondelle, and A. Olaya-Castro, *Chem. Sci.* **8**, 6871 (2017).
- [29] I. B. Juhász and A. I. Csurgay, *AIP Adv.* **8**, 045318 (2018).
- [30] H. C. H. Chan, O. E. Gamel, G. R. Fleming, and K. B. Whaley, *J. Phys. B* **51**, 054002 (2018).
- [31] O. J. Gómez-Sánchez and H. Y. Ramírez, *Phys. Rev. A* **98**, 053846 (2018).

- [32] L. Dong, C. Zhu, and H. Pu, *Atoms* **3**, 182 (2015).
- [33] M. Scala, B. Militello, A. Messina, J. Piilo, and S. Maniscalco, *Phys. Rev. A* **75**, 013811 (2007).
- [34] M. Scala, B. Militello, A. Messina, S. Maniscalco, J. Piilo, and K.-A. Suominen, *J. Phys. A* **40**, 14527 (2007).
- [35] G. G. Giusteri, F. Recrosi, G. Schaller, and G. L. Celardo, *Phys. Rev. E* **96**, 012113 (2017).
- [36] J. Kołodziej, J. B. Brask, M. Perarnau-Llobet, and B. Bylicka, *Phys. Rev. A* **97**, 062124 (2018).
- [37] M. T. Mitchison and M. B. Plenio, *New J. Phys.* **20**, 033005 (2018).
- [38] P. P. Hofer, M. Perarnau-Llobet, L. D. M. Miranda, G. Haack, R. Silva, J. B. Brask, and N. Brunner, *New J. Phys.* **19**, 123037 (2017).
- [39] J. O. Gonzalez, L. A. Correa, G. Nocerino, J. P. Palao, D. Alonso, and G. Adesso, *Open Syst. Inf. Dyn.*, **24**, 1740010 (2017).
- [40] J. Olšina, A. G. Dijkstra, C. Wang, and J. Cao, *arXiv*: 1408.5385.
- [41] J. del Pino, F. A. Y. N. Schröder, A. W. Chin, J. Feist, and F. J. Garcia-Vidal, *Phys. Rev. Lett.* **121**, 227401 (2018).
- [42] A. Garg, J. N. Onuchic, and V. Ambegaokar, *J. Chem. Phys.* **83**, 4491 (1985).
- [43] M. Thoss, H. Wang, and W. H. Miller, *J. Chem. Phys.* **115**, 2991 (2001).
- [44] H. J. Carmichael, *Statistical Methods in Quantum Optics 2: Non-Classical Fields* (Springer, New York, 2009).
- [45] A. G. Dijkstra and Y. Tanimura, *J. Chem. Phys.* **142**, 212423 (2015).
- [46] R. Loudon, *The Quantum Theory of Light* (Oxford University Press, Oxford, 2000).
- [47] H. -P. Breuer and F. Petruccione, *The Theory of Open Quantum Systems* (Oxford University Press, Oxford, 2002).
- [48] G. S. Agarwal, *Quantum Optics* (Cambridge University Press, Cambridge, England, 2013).
- [49] See Supplemental Material at <http://link.aps.org/supplemental/10.1103/PhysRevLett.123.093601> for further details.
- [50] J.-B. Trebbia, H. Ruf, P. Tamarat, and B. Lounis, *Opt. Express* **17**, 23986 (2009).
- [51] R. C. Schofield, K. D. Major, S. Grandi, S. Boissier, E. A. Hinds, and A. S. Clark, *J. Phys. Commun.* **2**, 115027 (2018).
- [52] R. L. De Sousa, J. L. Alves, and H. W. Alves, *Mater. Sci. Eng. C* **24**, 601 (2004).
- [53] J. Du, T. Teramoto, K. Nakata, E. Tokunaga, and T. Kobayashi, *Biophys. J.* **101**, 995 (2011).
- [54] E. Romero, R. Augulis, V. I. Novoderezhkin, M. Ferretti, J. Thieme, D. Zigmantas, and R. van Grondelle, *Nat. Phys.* **10**, 676 (2014).

*Correction:* Figures 2 and 3 contained plotting errors and have been replaced.